Available online at www.sciencedirect.com
SCIENCE DIRECT®
International Journal of Heat and Mass Transfer 47 (2004) 5011–5020
International Journal of HEAT and MASS TRANSFER
www.elsevier.com/locate/ijhmt

Simulation of phase states for water in nanoscale systems by molecular dynamics method

Chin-Hsiang Cheng *, Hsiu-Wen Chang

Department of Mechanical Engineering, Tatung University, 40 Chungshan N. Road, Sec. 3, Taipei, Taiwan 10451, ROC

Received 21 November 2003; received in revised form 25 June 2004
Available online 24 August 2004

Abstract

Molecular dynamics (MD) method is adopted to predict the kinematic behavior of water molecules in various equilibrium states. The range of states considered in the present simulation covers the saturated liquid–vapor mixture region, near-critical region, and supercritical region. Translational and angular velocities as well as the locations of all the molecules can be predicted at any instant when the inertial and external forces acting on the molecules have been determined. The interactive forces between molecules are determined based on Carravetta–Clementi (CC) potential. Based on the data of position and velocity vectors of the molecules at any instant, the variations in potential, kinetic, and total energies of the system during the simulation process toward equilibrium in an ⟨NVT⟩ or ⟨NVE⟩ ensemble are investigated, and some statistic quantities have been evaluated by ensemble averaging. The present simulation results for the near-critical region tend to confirm the data provided by Ohara and Aihara [S. Kotake, C.L. Tien (Ed.), Molecular and Microscale Heat Transfer, Begell House, New York, 1994, p. 132; Trans. JSME, Ser. B 60 (1994) 146].

Keywords: Molecular dynamics; Phase transition; CC potential; Water

1. Introduction

Molecular-level systems and models have been recognized to be more essential in the heat and mass transfer area. There has been much effort of extending the traditional macroscopic analysis to these extremely microscopic conditions in space (micrometer or even nanometer scale), time (nanosecond or even picosecond technology), and rate (extremely high heat flux). The molecular dynamics (MD) methods have long been used and are well developed as a tool in statistical mechanics and chemistry. However, it is a new challenge to extend the method to the spatial and temporal scale of microscopic heat transfer phenomena. The MD simulations could become viable as a tool for analyzing systems on a nanoscale level. Formulations of MD are deterministic and consist of simultaneously solving Newton's equations of motion for each atom, molecule, or system of molecules to determine properties of the materials. A detailed review about the MD method has been provided by Maruyama [1].

Fluids exhibit various phases at different states as a liquid, a vapor, or a liquid–vapor mixture depending on their temperature and pressure. The phase separation disappears at a temperature higher than its critical point.

* Corresponding author. Tel.: +886 02 2592 5252 3410; fax: +886 02 2599 7142.
E-mail address: cheng@ttu.edu.tw (C.-H. Cheng).

0017-9310/$ - see front matter © 2004 Elsevier Ltd. All rights reserved.
doi:10.1016/j.ijheatmasstransfer.2004.06.018

Nomenclature

a_1–a_4	CC potential parameters
b_1–b_4	CC potential parameters
c	molecule velocity
E	energy, J
$\boldsymbol{F}$	force vector, N
H	hydrogen atom
I	moment of inertia
k_B	Boltzmann constant
m	mass of a water molecule, kg
M	moment, N m/dummy point with negative charge
N	number density, m^{-3}
n	number of molecules
O	oxygen atom
P	pressure, Pa
q	electric charge
r	distance, m
$\boldsymbol{R}$	position vector
s	iteration step
T	temperature, K
t	time, ps
U	internal energy, J
V	volume, m^3
$\boldsymbol{v}$	velocity vector
u, v, w	velocity components

Greek symbols

Δt	time step
Φ	potential, J
ϕ	pair potential, J
ρ	density, kg/m^3
ω	angular velocity, rad/s

Subscripts

C	center of mass
H	Hydrogen
i, j	indices of water molecules
K	kinetic energy
M	dummy point with negative charge of $-2q$
O	Oxygen
P	potential energy
T	total energy
x, y, z	reference rectangular coordinates
1, 2, 3, 4	indices of hydrogen atoms
5, 6	indices of oxygen atoms
7, 8	indices of dummy points with negative charge

Near the critical point, physical properties such as specific heat and thermal conductivity vary markedly. The microscopic structure of fluid changes with phase and state, especially in the near-critical and supercritical regions. However, the structure changes have not been fully understood. Molecular dynamics simulation has been expected to be useful in the study of the microscopic structure of fluids. As a matter of fact, some analyses of the supercritical fluids can be found in the literature. Kataoka [2] performed MD simulations on water using the Carravetta–Clementi intermolecular potential (CC potential) model [3] and derived an equation of state at critical point. Radial distribution functions of supercritical water have been reported by Belonoshko and Saxena [4], Cummings et al. [5], and Guissani and Guillot [6] for some particular cases. Lately, Ohara and Aihara [7,8] adopted the CC potential to simulate water properties in the saturated liquid–vapor mixture region and the near-critical region. Microscopic information on the molecular structure and behavior, including the velocity auto-correlation and the formation of dimmers and clusters, was presented.

The effective pair potential for liquid water has been extensively studied in the past several decades. The ST2 potential proposed by Stillinger and Rahman [9] was widely used in 1980s. These authors modeled the potential function as the summation of Coulomb potential between charges and the Lennard–Jones potential between oxygen atoms. Lately, two much simpler forms of potential for water, the SPC potential and the SPC/E (extended SPC) potential, were introduced by Berendsen et al. [10,11]. Meanwhile, the TIP4P potential, which is regarded as one of the optimized potentials for liquid simulation, was developed by Jorgensen et al. [12,13]. In 1976, Matsuoka et al. [14] presented a potential which is applied for study of the water dimers. This model was then called MCY potential. Carravetta and Clementi [3] modified the MCY potential in accordance with experiments and proposed the CC potential. The CC potentials was based on ab initio quantum molecular calculations of water dimer with the elaborate treatment of electron correlation energy [1]. It is particularly suitable for the simulations of the structure of water dimers or clusters. A comparison among the CC, MCY, TIP4P, and SPC/E potentials are given in Fig. 1. The relative orientation of the water molecules in accordance with which the potentials are calculated is indicated in this figure. Note that when the relative orientation is changed, all the potentials shown in this figure will be altered.

In this study, the MD method is applied to simulate the microscopic structure of water and the interface properties at various states in a nanoscale system. The simulations have been performed for water over wide

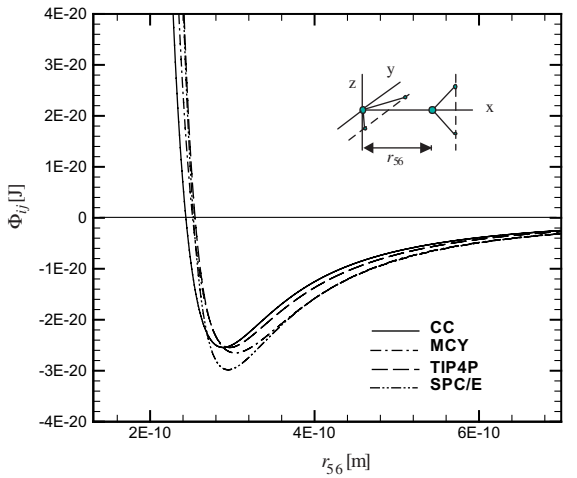

Fig. 1. A comparison among CC, MCY, TIP4P, and SPC/E potentials.

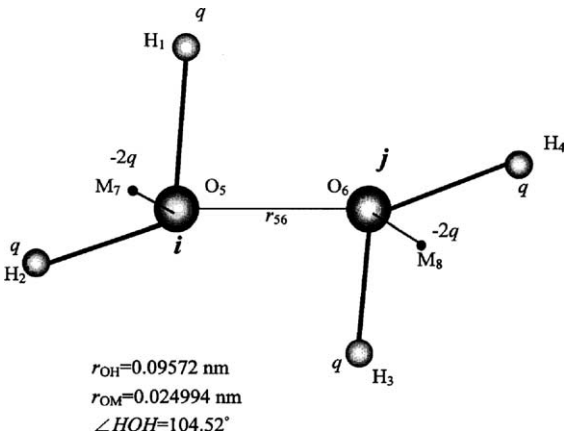

Fig. 2. Water molecules i and j.

ranges of temperature and density. The CC potential [3] is used to calculate the interactive force and potential energy among the water molecules. For each water molecule, the translational and angular velocities as well as the locations are predicted at any instant when the interactive force and the inertial force acting on the molecules are calculated. The interactive force between two water molecules involves the van der Waals force and the electrostatic force among hydrogen and oxygen atoms of the water molecules. Based on the obtained microscopic kinematic data, the variations in kinetic, potential, and total energy have been carried out, and several statistic quantities have been evaluated.

The microscopic behavior of water molecules in the near-critical and the saturated liquid–vapor mixture regions is of major concern. In an ⟨NVT⟩ ensemble, temperature control is performed during the simulation process toward equilibrium at a specified temperature. On the other hand, in an ⟨NVE⟩ ensemble, the variation in the total energy of the control system is monitored to check if the energy conservation is satisfied in the simulation process.

2. Molecular dynamics method

2.1. Equations of motion

In the molecular dynamics method, the motion of any molecule is determined by the Newton's second law of motion. Newton's second law of motion states that the time rate of change of the linear momentum of a molecule in an inertial coordinate system equals the net force acting on the molecule. That is

$$\boldsymbol{F}_i = m_i \frac{\mathrm{d}^2 \boldsymbol{r}_{ci}}{\mathrm{d}t^2} \tag{1}$$

where m_i, $\boldsymbol{r}_{ci}$, and $\boldsymbol{F}_i$ are the mass, position vector of mass center, and external force vector for molecule i, respectively.

A water molecule consists of one oxygen (O) and two hydrogen (H) atoms. A rigid water molecule is modeled as in Fig. 2, with $r_{\mathrm{OH}} = 0.09572$ nm and $\angle\mathrm{HOH} = 104.52°$. A hydrogen atom carries one positive charge of $0.18559e$ and an oxygen atom carries two negative charges. In this rigid water molecule model, a positive point charge q is attached on each hydrogen atom, whereas a negative charge of $-2q$ is placed on a virtual point (M) located at r_{OM} from the oxygen atom on the bisector of the angle $\angle$HOH. This model is referred to as a four-site model (O, H, H, and M) for water molecule. For the four-site model shown in Fig. 2, the effective pair potential Φ_{ij} between water molecules i and j is actually a function of the distances among the two sets of atoms and point charges. That is,

$$\Phi_{ij} = f(r_{13}, r_{14}, r_{16}, r_{18}, r_{23}, r_{24}, r_{26}, r_{28}, r_{35}, r_{37}, r_{45}, r_{47}, r_{56}, r_{78}) \tag{2}$$

where the indices 1, 2, 3, 4, 5, 6, 7, and 8 denote the sites of atoms or point charges H_1, H_2, H_3, H_4, O_5, O_6, M_7, and M_8.

On the other hand, the rotational motion of water molecule i is simulated based on the angular momentum equation of motion

$$\boldsymbol{M}_i = \frac{\mathrm{d}\boldsymbol{H}_i}{\mathrm{d}t} \tag{3}$$

where $\boldsymbol{M}_i$ and $\boldsymbol{H}_i$ are the moment and the angular momentum vectors, respectively, of molecule i, and

$$\begin{aligned} \boldsymbol{M}_i &= \boldsymbol{r}_{cl} \times \boldsymbol{F}_l \quad (l = 1, 2, 5, 7) \\ &= \boldsymbol{M}_{xi}\vec{\boldsymbol{i}} + \boldsymbol{M}_{yi}\vec{\boldsymbol{j}} + \boldsymbol{M}_{zi}\vec{\boldsymbol{k}} \end{aligned} \tag{4}$$

where $\mathbf{r}_{cl}$ represents the relative position vector between atom l (or point charges) and the mass center of molecule i. When expressed in a reference rectangular coordinate (x,y,z) of which the origin is fixed at the mass center of molecule i and the three axes coincide with the three principle axes of the mass system of molecule i, the angular momentum equation leads to

$$M_{xi} = I_{xx}\dot{\omega}_x - (I_{yy} - I_{zz})\omega_y\omega_z \tag{5a}$$

$$M_{yi} = I_{yy}\dot{\omega}_y - (I_{zz} - I_{xx})\omega_z\omega_x \tag{5b}$$

$$M_{zi} = I_{zz}\dot{\omega}_z - (I_{xx} - I_{yy})\omega_x\omega_y \tag{5c}$$

where ω_x, ω_y, ω_z are the components of the angular velocity vector and I_{xx}, I_{yy}, I_{zz} denote the moment of inertia, with respect to the reference coordinate. It is noticed that the obtained angular velocity components ω_x, ω_y, and ω_z at each instant should be transformed into the angular velocity components associated with the inertial coordinate frame for calculating the position coordinates for the molecules. Note that $\dot{\omega}_x = \mathrm{d}\omega_x/\mathrm{d}t$, $\dot{\omega}_y = \mathrm{d}\omega_y/\mathrm{d}t$, and $\dot{\omega}_z = \mathrm{d}\omega_z/\mathrm{d}t$. Therefore, Eqs. (5a)–(5c) represent three simultaneous 1st-order ordinary differential equations. As long as the angular velocity components ω_x, ω_y, and ω_z at an initial time $t = t_0$ are known, these components at $t = t_0 + \Delta t$ can be calculated using Eqs. (5a)–(5c) by numerical integration with respect to time.

2.2. Numerical simulation

The integration of the equations of motion is straightforward, and a simpler integration scheme is usually preferred in MD analysis. In the present study, Verlet's integration scheme [15] is used to solve the equation of motion, Eq. (1) by numerical integration. On the other hand, finite difference method can be applied for the angular momentum equations, Eqs. (5a)–(5c). An iterative procedure is required to solve ω_x, ω_y, and ω_z simultaneously at each time step, coupled with the finite difference method. Convergence criterion of the iterative procedure is set by

$$|(A^{s+1} - A^s)/A^s| \leqslant 10^{-4} \tag{6}$$

where A represents ω_x, ω_y, or ω_z, and s is the iteration number.

In the present MD analysis, all the faces of the control volume are specified by a periodic boundary condition. The simulations are performed for a system of 256 or 320 water molecules in a cubic control volume (V). The number of molecules selected in this study is equal to that used by Ohara and Aihara [7,8] such that the present results may be used to fairly verify these existing reports. Initially, the molecules are placed to form a f.c.c. crystal structure with randomly directed velocity. Typically, calculations in overall 220,000 time steps were performed at $\Delta t = 2.5 \times 10^{-16}$ s. The ensemble averages are calculated after the 120,000th time step. In general, it takes 30–40 h to complete the computation for a case from the initial configuration to the final equilibrium state when the computation is excused on a PentiumIII-800 MHz personal computer.

2.3. Carravetta–Clemeni (CC) potential

The CC potential [3] is expressed as

$$\begin{aligned}\Phi_{ij} = {} & q^2\left(\frac{1}{r_{13}} + \frac{1}{r_{14}} + \frac{1}{r_{23}} + \frac{1}{r_{24}}\right) + \frac{4q^2}{r_{78}} \\ & - 2q^2\left(\frac{1}{r_{18}} + \frac{1}{r_{28}} + \frac{1}{r_{37}} + \frac{1}{r_{47}}\right) + a_1\exp(-b_1 r_{56}) \\ & + a_2[\exp(-b_2 r_{13}) + \exp(-b_2 r_{14}) + \exp(-b_2 r_{23}) \\ & + \exp(-b_2 r_{24})] + a_3[\exp(-b_3 r_{16}) + \exp(-b_3 r_{26}) \\ & + \exp(-b_3 r_{35}) + \exp(-b_3 r_{45})] - a_4[\exp(-b_4 r_{16}) \\ & + \exp(-b_4 r_{26}) + \exp(-b_4 r_{35}) + \exp(-b_4 r_{45})]\end{aligned} \tag{7}$$

where

$$\begin{aligned} q^2 &= 0.998565 \times 10^{-28}\ (\mathrm{J\,m}) \\ a_1 &= 3157.08 \times 10^{-18}\ (\mathrm{J}) \\ a_2 &= 24.8732 \times 10^{-18}\ (\mathrm{J}) \\ a_3 &= 14.6940 \times 10^{-18}\ (\mathrm{J}) \\ a_4 &= 3.18140 \times 10^{-18}\ (\mathrm{J}) \\ b_1 &= 4.7555 \times 10^{10}\ (\mathrm{m^{-1}}) \\ b_2 &= 3.8446 \times 10^{10}\ (\mathrm{m^{-1}}) \\ b_3 &= 3.1763 \times 10^{10}\ (\mathrm{m^{-1}}) \\ b_4 &= 2.4806 \times 10^{10}\ (\mathrm{m^{-1}}) \end{aligned} \tag{8}$$

and r_{13}, r_{14}, r_{16}, r_{18}, r_{23}, r_{24}, r_{26}, r_{28}, r_{35}, r_{37}, r_{45}, r_{47}, r_{56}, r_{78} are the distances between the atoms or point charges of molecules i and j, which are shown in Fig. 2. The intermolecular potential of water molecules is reasonably expressed by this function.

2.4. System energies

In a nonreactive molecular system, the total energy (E_T) is defined as the sum of all microscopic forms of energy of a system. It is related to molecular structure and degree of molecular activity and may be viewed as the sum of the kinetic and potential energies of the molecules. The water molecules move in the control volume with different velocities, and thus possess different kinetic energies. This is known as the translational kinetic energy. In the mean time, each of the atoms of a water molecule rotates about the axis passing through the mass center of the molecule, and the energy associated with this rotation is the rotational kinetic energy. The atoms of the water molecules may also vibrate about

their common mass centers, the energy associated with this back-and-forth motion is the vibrational kinetic energy. For water molecules the kinetic energy is mostly due to the translational and rotational motions and the vibration motion becoming appreciable only at very higher temperature. Therefore, in this study the vibrational kinetic energy is neglected.

The potential, kinetic, and total energies of a molecular system are defined as follows:

(1) *Potential energy* (E_P)

$$E_P = \sum_i \sum_{j \geqslant i} \Phi_{ij} \tag{9}$$

where the potential between water molecules i and j, Φ_{ij}, is calculated with the CC potential expressed in Eq. (7).

(2) *Kinetic energy* (E_K)

Kinetic energy of molecules includes the translational and rotational kinetic energies of molecules (E_{KT} and E_{KR}). The kinetic energy (E_K) is determined by

$$E_K = E_{KT} + E_{KR} \tag{10}$$

(3) *Total energy* (E_T)

Total energy of the system is the summation of potential energy and kinetic energy, i.e.

$$E_T = E_P + E_K \tag{11}$$

In addition, the pair-distribution function $g(r)$ and the velocity autocorrelation function $\langle \boldsymbol{v}(0) \cdot \boldsymbol{v}(t) \rangle$ are evaluated. Note that $\langle \boldsymbol{v}(0) \cdot \boldsymbol{v}(t) \rangle$ is a time-dependent correlation and $g(r)$ is time-independent. The definitions of these statistical quantities are given in the following:

(1) *Pair-distribution function* $g(r)$

Let $n(r)$ be the number of molecules located within r and $r + \Delta r$ from a selected molecule. The pair-distribution function is defined by

$$g(r) = (V/N)[n(r)/(4\pi r^2 \Delta r)] \tag{12}$$

Note that for a gas, with a long-term average, the pair-distribution function is independent of the molecule selected. However, for a solid crystal, $g(r)$ may exhibit different features related to different selected molecules. In calculation for $g(r)$, locations of the water molecules are represented by the locations of the mass centers.

(2) *Velocity autocorrelation function* $\langle \boldsymbol{v}(0) \cdot \boldsymbol{v}(t) \rangle$

$$\langle \boldsymbol{v}(0) \cdot \boldsymbol{v}(t) \rangle = \frac{1}{N} \sum_{i=1}^{N} \boldsymbol{v}_{ci}(0) \cdot \boldsymbol{v}_{ci}(t) \tag{13}$$

When calculating the time-dependent correlation, $\langle \boldsymbol{v}(0) \cdot \boldsymbol{v}(t) \rangle$, one may treat any time instant as a time origin, and an ensemble average can be evaluated for a large number (say, 100) of sampling periods starting from different time origins.

The distribution of velocity is evaluated based on the velocity data of the mass centers of the molecules. In equilibrium states, the distribution of velocity approaches the Maxwell–Boltzmann distribution, which is

$$f(c) = \left(\frac{m}{2\pi k_B T}\right)^{2/3} \exp\left(-\frac{mc^2}{2k_B T}\right) \tag{14}$$

where $c = \sqrt{u_c^2 + v_c^2 + w_c^2}$ and u_c, v_c and w_c denote the components of velocity vectors of mass centers of molecules. A comparison between the present computation results and Eq. (14) has been made, and close agreement has been observed.

3. Results and discussion

The states simulated in the present study cover the saturated liquid–vapor mixture, near-critical, and supercritical regions. Table 1 provides the cases studied in this report. These studied cases are also shown on the P–V diagram of water (Fig. 3) to illustrate their states and the regions in which they are located.

3.1. Numerical checks

Considering the near-critical region, Ohara and Aihara [7,8] presented the MD simulation results for the configurations of water molecules and the statistical quantities at various temperature and density. The states of the cases studied by Ohara and Aihara [7,8] are indicated in Table 1. In this report, parts of the results are compared with the information presented by Ohara and Aihara [7,8]. Fig. 4 shows the results for the velocity autocorrelation function as a function of time at $\rho = 380$ kg/m^3 and $T = 300$, 492, and 793 K. The data provided by Ohara and Aihara [7] are also given for

Table 1
Cases studied

Case	T (K)	ρ (kg/m^3)	Remark
1	300	380	[7]
2	492	380	[7]
3	793	380	[7]
4	300	300	[8]
5	600	300	[8]
6	850	300	[8]
7	300	30.6	
8	373	30.6	
9	473	30.6	
10	603	30.6	
11	300	500	
12	373	500	
13	473	500	
14	638	500	
15	473	100	
16	473	50	

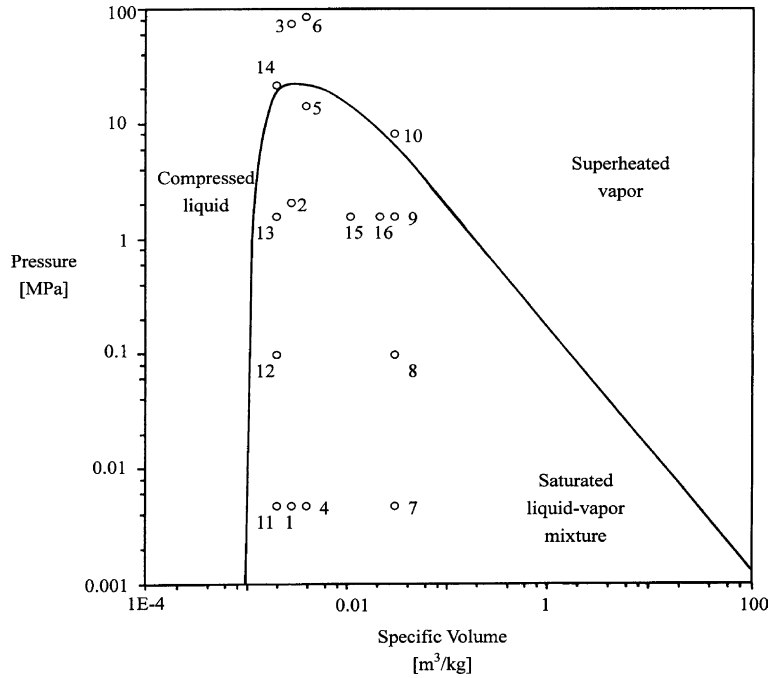

Fig. 3. States of studied cases on P–V diagram.

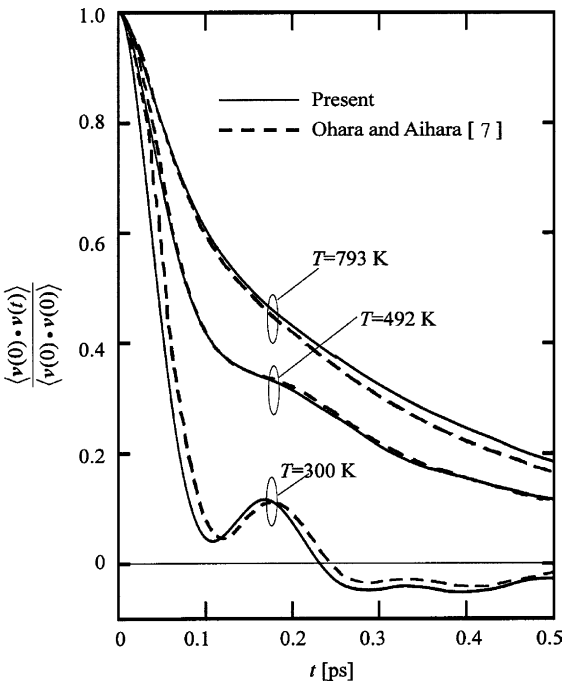

Fig. 4. Velocity autocorrelation function as a function of time for water at $\rho = 380$ kg/m^3 and $T = 300$, 492, and 793 K.

comparison. The results are presented in terms of $\langle \boldsymbol{v}(0) \cdot \boldsymbol{v}(t) \rangle / \langle \boldsymbol{v}(0) \cdot \boldsymbol{v}(0) \rangle$. It is found that at $T = 300$ K, the velocity autocorrelation function becomes negative at about $t = 0.23$ ps. However, at a higher temperature, the velocity autocorrelation function is always positive. It is observed that both two sets of curves exhibit very similar trend. Note that the slight discrepancy between these two sets of data may be further reduced as more periods of sampling are brought into ensemble average.

Fig. 5 shows the results for the pair distribution function $g(r)$ in comparison with the information provided by Ohara and Aihara [8]. It is found that the pair distribution function attains a maximum (first-neighbor peak) at approximately $r_{ij} = 0.3$ nm. This indicates that local number density reaches a maximum at such a distance from any selected molecule. It is seen that even at $T = 850$ K, the remnant of the first-neighbor peak is still visible. According to the comparisons shown in Figs. 4 and 5, it is found that the present simulation results for the near-critical region tend to confirm the data provided by Ohara and Aihara [7,8].

The location of the first-neighbor peak can be expected when the potential and the pair distribution function are shown together. As illustrated in Fig. 6, it is clearly seen that the location of the first-neighbor peak of $g(r)$ is right at the point of minimum potential. Since a minimum potential leads to a most stable distance between two molecules, it is natural that local number density of molecules reaches a maximum there.

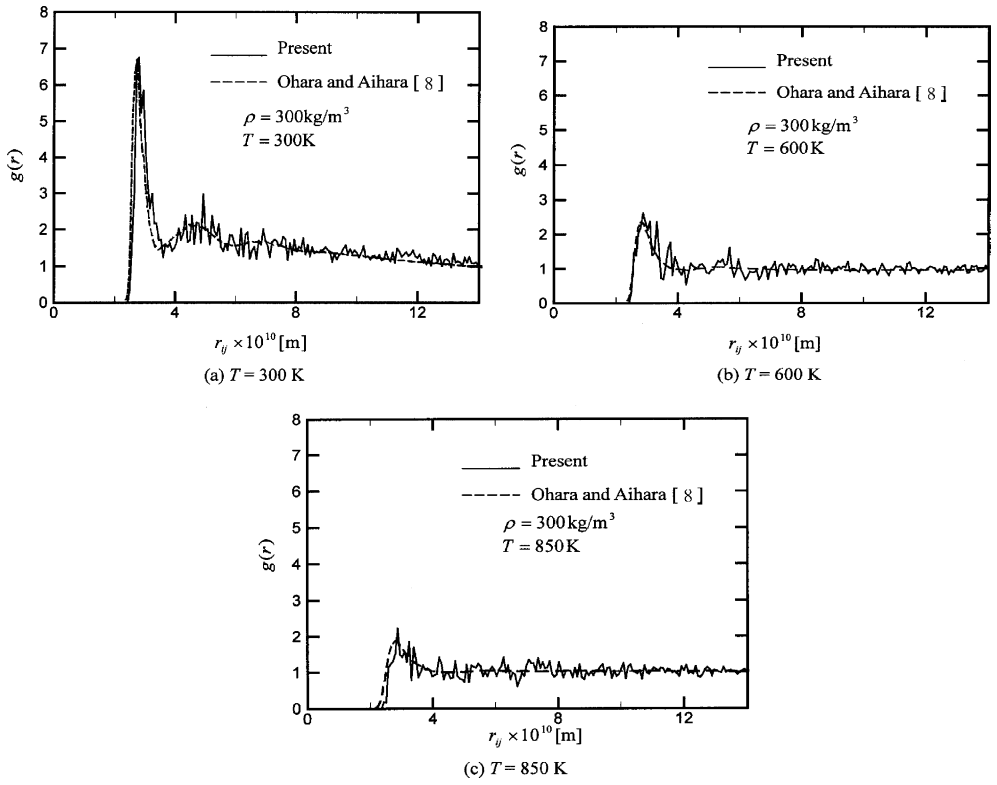

Fig. 5. Pair distribution function for water at $\rho = 300$ kg/m^3 and $T = 300$, 600, and 850 K.

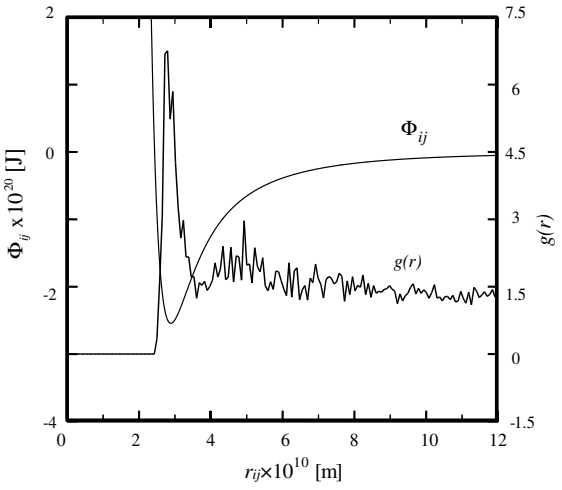

Fig. 6. Relationship between potential and pair distribution function, for water at $\rho = 300$ kg/m^3 and $T = 300$ K.

3.2. Phase states of water

The temperature and density of water are varied to specify various states. Fig. 7 shows the configuration of molecules at various equilibrium states. The states of the cases displayed in this figure are already indicated in Table 1 and Fig. 3. As indicated in Fig. 3, the cases are scattered in the saturated liquid–vapor mixture, near-critical, and supercritical regions. Snapshots of the configurations of water molecules at various equilibrium states are presented in Fig. 7. Fig. 7(a) and (b) shows the water droplets formed by the molecules for cases 7 and 8. The water state now is in the saturated liquid–vapor mixture region with a higher quality. However, when the temperature is further increased, as in cases 9 and 10 in Fig. 7(c) and (d), the droplets turn to cluster of molecules and eventually vaporize to be the superheated vapor. It is seen in Fig. 7(d) that with case 10 the control volume is full of free molecules of the vapor phase.

Cases 11–14 are of higher density $\rho = 500$ kg/m^3. Thus, in Fig. 7(e)–(h), the configurations of molecules for the states of lower quality can be observed. It is found that the control volume is nearly occupied by a region of high number density, any only a few free molecules are traveling in the empty spaces in the control volume. Note that case 14 is located in the compressed-liquid region close to the critical point.

Based on the results for cases 13, 15, 16, and 9, one can observe the phase transition from liquid to vapor at constant pressure. It has been seen that the control

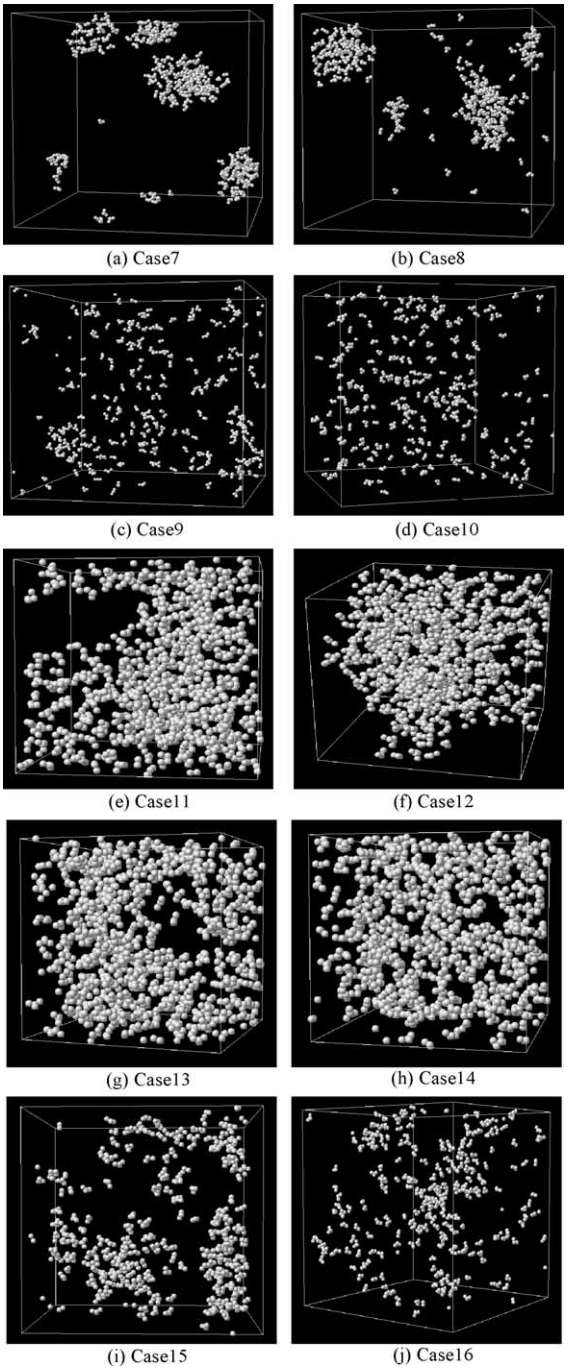

Fig. 7. Snapshots of configurations of water molecules at various equilibrium states.

volume is nearly occupied by the liquid phase for case 13 shown in Fig. 7(g). When the specific volume is increased, more molecules are vaporized from the liquid region as in cases 15 and 16. The liquid region continues

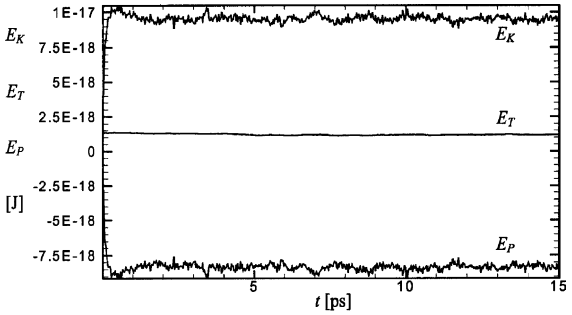

(a) Variations in potential, kinetic, and total energies.

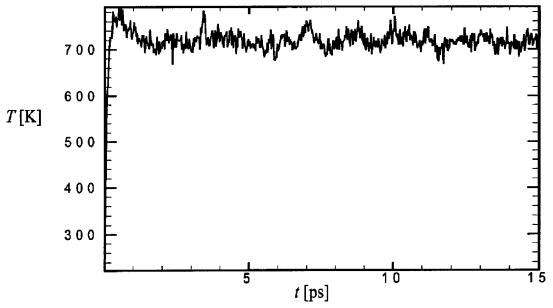

(b) Variations in system temperature.

Fig. 8. Energy conservation in the process from initial state to equilibrium state for ⟨NVE⟩ ensemble, at $\rho = 380$ kg/m^3.

to shrink if the specific volume is further increased, and eventually in case 9 only clusters of water molecules are found and the control volume is nearly full of the free molecules of vapor phase. In accordance with the results presented in Fig. 7, it is found that the simulations of the phase states by the MD method coincide with the physical behavior of water at various states.

Fig. 8 shows the energy conservation for an ⟨NVE⟩ ensemble with 256 molecules in the control volume at $\rho = 380$ kg/m^3. Two plots are provided in this figure. Fig. 8(a) displays the variations in the potential, kinetic, and total energies. It is found that in the simulation process a decrease in the potential energy is always accompanied by an increase in the kinetic energy, and vice versa. Therefore, the total energy is always kept constant even though the energy may change its forms between the potential and the kinetic energies. The variation in system temperature is conveyed in Fig. 8(b). It is observed that the system eventually approaches an equilibrium temperature of approximately 720 K. The variation in system temperature is clearly in resonance with the variation in the kinetic energy as expected.

Fig. 9 conveys the variations in the potential, kinetic, and total energies and system temperature for an ⟨NVT⟩ ensemble with temperature control. One must be aware

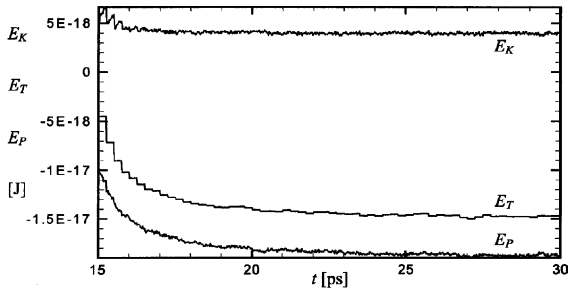

(a) Variations in potential, kinetic, and total energies.

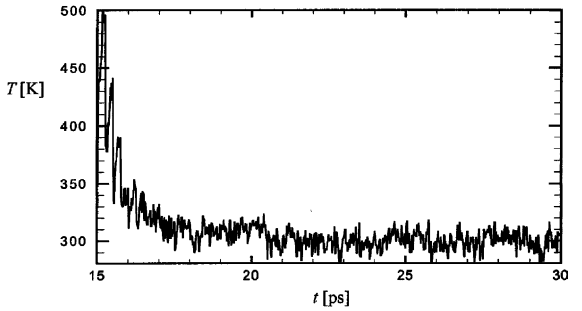

(b) Variations in system temperature.

Fig. 9. Energy variation in process from initial state to equilibrium state for ⟨NVT⟩ ensemble under temperature control $T = 300$ K, for water at $\rho = 380$ kg/m^3.

that the kinetic energy of molecules is artificially adjusted due to temperature control, and thus the total energy of the system is varied. In Fig. 9(a), the zig-zag variations found on the curves for E_K and E_T indicate the influence of temperature control. The temperature of the system is readily reduced to the desired temperature of $T = 300$ K in 20 ps by the temperature control for this case.

4. Concluding remarks

The range of states considered in the present simulation covers the saturated liquid–vapor mixture, near-critical, and supercritical regions. Meanwhile, close agreement of the present results has been found with the data provided by Ohara and Aihara [7,8]. Therefore, the data provided by Ohara and Aihara [7,8] have been confirmed.

Results for the phase configuration of water molecules at various equilibrium states are provided. The phase state at various equilibrium states is studied, and the formation of liquid layer, droplets, clusters, and vapor phase is observed. It is found that the simulations of the phase states by the MD method coincide with the physical behavior of water at various states. Meanwhile, the variations in potential, kinetic, and total energies during the simulation process toward equilibrium in an ⟨NVT⟩ or ⟨NVE⟩ ensemble are clearly observed.

Acknowledgments

The study is supported by the National Science Council of Taiwan, the Republic of China through the grant NSC91-2212-E-036-004. Partial support of this study by Tatung University under grant B91-M05-033 is also appreciated. Visualization of molecules is performed by using a MD visualization program (pvwin.exe), which is kindly provided by Professor Shigeo Maruyama of Department of Mechanical Engineering, The University of Tokyo.

References

[1] S. Maruyama, Molecular dynamics method for microscale heat transfer, in: W.J. Minkowycz, E.M. Sparrow (Eds.), Advances in Numerical Heat Transfer, vol. 2, Taylor & Francis, New York, 2000, pp. 189–226 (Chapter 6).
[2] Y. Kataoka, Studies of liquid water by computer simulations. V. Equation of state of fluid water with Carravetta–Clementi potential, J. Chem. Phys. 87 (1987) 589–598.
[3] V. Carravetta, E. Clementi, Water–water interaction potential: an approximation of the electron correlation contribution by a function of the SCF density matrix, J. Chem. Phys. 81 (1984) 2646–2651.
[4] A. Belonoshko, S.K. Saxena, A molecular dynamics study of the pressure–volume–temperature properties of supercritical fluids: I. H_2O, Geochim. Cosmochim. Acta 55 (1991) 381–387.
[5] P.T. Cummings, H.D. Cochran, J.M. Simonson, R.E. Mesmer, S. Karabomi, Simulation of supercritical water and of supercritical aqueous solutions, J. Chem. Phys. 94 (1991) 5606–5621.
[6] Y. Guissani, B. Guillot, A computer simulation study of the liquid–vapor coexistence curve of water, J. Chem. Phys. 98 (1993) 8221–8235.
[7] T. Ohara, T. Aihara, Molecular dynamics study on structure of near-critical water, in: S. Kotake, C.L. Tien (Eds.), Molecular and Microscale Heat Transfer, Begell House, New York, 1994, pp. 132–137.
[8] T. Ohara, T. Aihara, Molecular dynamics study on cluster structure of water, Trans. JSME, Ser. B 60 (1994) 146–153 (in Japenese).
[9] F.H. Stillinger, A. Rahman, Improved simulation of liquid water by molecular dynamics, J. Chem. Phys. 60 (1974) 1545–1557.
[10] H.J.C. Berendsen, J.P.M. Postma, W.F. van Gunsteren, J. Hermans, in: B. Pullmann (Ed.), Intermolecular Forces, Reidel, Dordrecht, 1981, pp. 331–340.
[11] H.J.C. Berendsen, J.R. Grigera, T.P. Straatsma, The missing term in effective pair potentials, J. Phys. Chem. 91 (1987) 6269–6271.
[12] W.L. Jorgensen, J. Chandrasekhar, J.D. Madura, R.W. Impey, M.L. Klein, Comparison of simple potential

functions for simulating liquid water, J. Chem. Phys. 79 (1983) 926–935.
[13] W.L. Jorgensen, Optimized intermolecular potential functions for liquid alcohols, J. Phys. Chem. 90 (1986) 1276–1284.
[14] O. Matsuoka, E. Clementi, M. Yoshimine, CI study of the water dimer potential surface, J. Chem. Phys. 64 (1976) 1351–1361.
[15] M.P. Allen, D.J. Tildesley, Computer Simulation of Liquids, Oxford University Press, New York, 1987.